

# Non-Hermitian quantum geometric tensor and nonlinear electrical response

Kai Chen<sup>x</sup> and Jie Zhu<sup>+</sup>

*School of Physics Science and Engineering, Tongji University, Shanghai, China*

(Dated: September 16, 2025)

We demonstrate that the non-Hermitian quantum geometric tensor (QGT) governs nonlinear electrical responses in systems with a spectral line gap. The quantum metric, which is a component of the QGT and takes complex values in non-Hermitian systems, generates an intrinsic nonlinear conductivity independent of the scattering time, while the complex Berry curvature induces a wavepacket-width-dependent response. Using one-dimensional and two-dimensional non-Hermitian models, we establish a universal link between nonlinear dynamics and the QGT, thereby connecting quantum state geometry to observable transport phenomena. Crucially, our analysis indicates that the wavepacket width significantly affects non-Hermitian transport—a feature absent in Hermitian systems. This framework unifies non-Hermitian response theory by revealing how geometric degrees of freedom encode transport in open and synthetic quantum matter. Our results bridge fundamental quantum geometry with emergent functionality, offering pathways to exploit geometric effects in topological devices and engineered materials.

*Introduction.*—Higher-order responses play a crucial role in condensed matter physics, as they often reveal connections to emerging physical concepts. One prominent example is the QGT, which characterizes the geometric structure of quantum states in projective Hilbert space [1–3] and influences a system’s nonlinear response to external driving fields.

The QGT consists of two key components: its imaginary part, known as the Berry curvature [4], and its real part, the Fubini-Study quantum metric (QM) [5, 6]. The Berry curvature is central to various physical phenomena, including the quantum anomalous Hall effect [7, 8], topological insulators and superconductors [9, 10], Weyl and Dirac semimetals [11–14], orbital magnetization [15–17], and the converse vortical effect [18]. Meanwhile, the QM serves as the unique Riemannian metric in projective Hilbert space that remains invariant under unitary transformations. In Hermitian systems, the semipositive [1] nature of the QGT imposes constraints on the trace and determinant of its real and imaginary parts, leading to important physical inequalities [3, 19].

Recent interest in the QGT has surged, largely due to its role in material properties and the discovery of flat-band superconductivity in twisted materials [20–25]. Since then, numerous QGT-related phenomena have been (re)discovered, further expanding the field. For instance, the QM has been found to contribute to superfluid weight [26–30], optical conductivity [31, 32], nonlinear conductivity [33, 34], nonlinear transport [35–37] and the nonlinear quantum valley Hall effect [38]. As research continues, the study of the QGT remains a rich and evolving topic in condensed matter physics.

Non-Hermitian systems exhibit remarkable properties that distinguish them from their Hermitian counterparts [39, 40]. A defining feature is the skin effect [41, 42], where eigenstates localize exponentially at boundaries due to extreme sensitivity to boundary conditions, fundamentally altering spectral behavior. Another hallmark is the

emergence of non-Hermitian exceptional points [43, 44], spectral singularities at which eigenvalues and eigenvectors coalesce, collapsing the Hilbert space and enabling exotic phase transitions. Non-Hermiticity also modifies foundational frameworks such as linear response theory and transport phenomena [45–47], leading to counterintuitive effects absent in Hermitian systems. These phenomena, including unidirectional invisibility and enhanced sensitivity, lack direct analogs in Hermitian physics, underscoring the unique theoretical and experimental implications of non-Hermitian theories.

A crucial distinction in non-Hermitian systems arises from the difference between complex conjugation and transposition, which makes their symmetry structure more intricate [48, 49]. This added complexity extends the 10-fold way topological classification [50], originally formulated for Hermitian systems, into a broader 38-fold Bernard-LeClair class that accounts for non-Hermitian symmetries [48, 51, 52]. Furthermore, the complex nature of the energy spectrum necessitates a refined definition of band gaps. Unlike in Hermitian systems, non-Hermitian band gaps can be categorized as point or line gaps [44, 53], both of which play a crucial role in the topological classification of non-Hermitian phases.

In this work, we investigate the role of the non-Hermitian QGT in line-gapped non-Hermitian systems and its impact on nonlinear conductivity induced by an external electric field. Although line-gapped non-Hermitian systems are topologically equivalent to Hermitian systems [54]—as they can be adiabatically connected to a Hermitian limit—we demonstrate that they exhibit unique nonlinear responses absent in Hermitian systems. This distinction stems from the complex structure of the QGT in non-Hermitian systems, which fundamentally alters the mechanism of nonlinear conductivity compared to Hermitian cases. Specifically, we show that the complex QM and Berry curvature induce a contribution to the second-order nonlinear DC conductivity (SODCC) pro-

portional to the wavepacket width, a feature exclusive to non-Hermitian systems.

Furthermore, we analyze subsystems faithfully described by non-Hermitian Hamiltonians, which emerge due to interactions with their environment. As a paradigmatic example, we compute the nonlinear surface conductivity of a Chern insulator and isolate the distinct contributions of the QGT to this response.

Our findings underscore the critical role of quantum geometric structures in non-Hermitian systems, revealing novel physical properties and nonlinear transport phenomena with no Hermitian analogs.

*Nonlinear DC conductivity and QGT* — A fundamental distinction between non-Hermitian and Hermitian systems is that, in non-Hermitian systems, the left and right eigenstates of the Hamiltonian are different. These eigenstates satisfy the biorthogonality condition  $\langle \psi_{m,\mathbf{k}}^L | \psi_{n,\mathbf{k}}^R \rangle = \delta_{mn}$ , where  $\mathbf{k}$  denotes the Bloch momentum and  $m, n$  label the band indices. Specifically, for a non-Hermitian Hamiltonian  $H_{\text{NH}}(\mathbf{k})$ , the right eigenstates  $|\psi_{i,\mathbf{k}}^R\rangle$  and left eigenstates  $\langle \psi_{i,\mathbf{k}}^L|$  satisfy the eigenvalue equations  $H_{\text{NH}}(\mathbf{k})|\psi_{i,\mathbf{k}}^R\rangle = \xi_{i,\mathbf{k}}|\psi_{i,\mathbf{k}}^R\rangle$  and  $\langle \psi_{i,\mathbf{k}}^L|H_{\text{NH}}(\mathbf{k}) = \xi_{i,\mathbf{k}}\langle \psi_{i,\mathbf{k}}^L|$ , where  $\xi_{i,\mathbf{k}} \in \mathbb{C}$  is the complex energy, and resolve the identity operator as  $I = \sum_i |\psi_{i,\mathbf{k}}^R\rangle\langle \psi_{i,\mathbf{k}}^L|$ . Motivated by this distinction, we define operator expectations in the left-right basis as  $\langle \psi^L | \hat{O} | \psi^R \rangle$  for any operator  $\hat{O}$ .

In this section, we investigate how the non-Hermitian QGT governs the nonlinear DC conductivity. To establish this connection, we adopt a semiclassical framework, where the current density is given by  $\mathbf{J} = -e \int_{\mathbf{k}} f \dot{\mathbf{r}}$ , with  $\int_{\mathbf{k}} \equiv \int \frac{d^D k}{(2\pi)^D}$  denoting momentum-space integration in a  $D$ -dimensional system. Here,  $\dot{\mathbf{r}}$  represents the semiclassical electron velocity, and  $f$  is the distribution function.

The generalized semiclassical equations of motion for non-Hermitian systems under an external electric field  $\mathbf{E}$  are given by [55]:  $\dot{\mathbf{r}} = \text{Re}[\nabla_{\mathbf{k}}\xi_{n,\mathbf{k}} + e\mathbf{E} \times \boldsymbol{\Omega}_{n,\mathbf{k}}]$ ,  $\dot{\mathbf{k}} = -e\mathbf{E} + W^2 \text{Im}[\nabla_{\mathbf{k}}\xi_{n,\mathbf{k}} + e\mathbf{E} \times \boldsymbol{\Omega}_{n,\mathbf{k}}]$ , where  $e$  denotes the electron charge,  $W$  represents the Gaussian wave-packet width, and  $\text{Re}(\cdot)/\text{Im}(\cdot)$  extract the real/imaginary parts of  $\cdot$ . The non-Hermitian Berry curvature is defined as  $\boldsymbol{\Omega}_{n,\mathbf{k}} \equiv i\nabla_{\mathbf{k}} \times \langle \psi_{n,\mathbf{k}}^L | \nabla_{\mathbf{k}} \psi_{n,\mathbf{k}}^R \rangle$ . In the Hermitian limit, both the eigenvalues and the Berry curvature are real, and the semiclassical equations of motion reduce to their standard form in Hermitian systems [17].

To analyze the response of this system to a perturbative potential of the form  $-e\mathbf{E} \cdot \mathbf{r}$ . The high-order response of the current to an electric field can be extracted using the Schrieffer-Wolff transformation, which was applied in Ref. [36, 56] to study high-order responses in Hermitian systems. In the weak-field limit, expanding the distribution function  $f$ , group velocity  $\dot{\mathbf{r}}$ , band dispersion  $\xi_{\mathbf{k}}$ , and Berry curvature  $\boldsymbol{\Omega}_{\mathbf{k}}$  in powers of the external field  $\mathbf{E}$  allows, in principle, for obtaining the response to all orders in  $\mathbf{E}$  [see Appendix A for details]. In this work, we focus on the SODCc.

In the narrow wavepacket width limit, part of the semiclassical equations of motion simplifies to  $\mathbf{k} = -e\mathbf{E}$ . The SODCc is given by (see Appendix A for details):

$$\begin{aligned} \sigma_{\theta\mu\nu} = & -e^3 \int_{\mathbf{k}} \left\{ \tau^2 \text{Re} \left( \partial_{\theta} \xi_{\mathbf{k}}^{(0)} \right) \partial_{\mu} \partial_{\nu} f_0 \right. \\ & - \tau f_0 \frac{\epsilon_{\theta\mu l} \partial_{\nu} \text{Re} \Omega_l^{(0)} + \epsilon_{\theta\nu l} \partial_{\mu} \text{Re} \Omega_l^{(0)}}{2} \\ & \left. + f_0 \text{Re} \left( 2 \partial_{\theta} G_{\mu\nu}^{LR(0)} - \frac{\partial_{\nu} G_{\mu\theta}^{LR(0)} + \partial_{\mu} G_{\nu\theta}^{LR(0)}}{2} \right) \right\}, \end{aligned} \quad (1)$$

where we suppress the band index to simplify the notation, the indices  $\theta, \mu$ , and  $\nu$  label the spatial directions, and  $\epsilon_{\mu\nu\theta}$  is the antisymmetric Levi-Civita symbol. Here,  $\tau$  represents the scattering time, and  $f_0 = \left(1 + \exp^{\text{Re}\xi_{\mathbf{k}}^{(0)}/k_B T}\right)^{-1}$  is the equilibrium distribution function in the absence of external fields, as indicated by the superscript (0). Throughout this work, we set the Boltzmann constant  $k_B = 1$  and the electron charge  $e = 1$ . The third term in Eq. (1) is independent of the scattering time and is proportional to the band-renormalized non-Hermitian QM, which is defined as  $G_{\mu\nu}^{LR(0)} \equiv G_{n,\mu\nu}^{LR(0)} = \sum_{m \neq n} \frac{A_{nm,\mu}^{LR(0)} A_{mn,\nu}^{LR(0)} + A_{nm,\nu}^{LR(0)} A_{mn,\mu}^{LR(0)}}{2(\xi_{n,\mathbf{k}}^{(0)} - \xi_{m,\mathbf{k}}^{(0)})}$ , where  $n$  denotes the target band. The unperturbed non-Hermitian Berry connection is given by  $A_{mn,\mu}^{LR(0)} \equiv i \langle \psi_{m,\mathbf{k}}^L | \partial_{\mu} \psi_{n,\mathbf{k}}^R \rangle$ , and the unperturbed non-Hermitian Berry curvature is  $\boldsymbol{\Omega}^{(0)} \equiv i \nabla_{\mathbf{k}} \times \mathbf{A}_{nn}^{LR(0)}$ . Interestingly, without applying the real part operation in Eq. (1), the expression takes the same form as in the Hermitian system [56]. However, non-Hermiticity generally leads to a complex QM. As a result, Eq. (1) introduces essential differences from its Hermitian counterpart, reflecting the influence of non-Hermitian effects on the system.

*Non-Hermitian Su-Schrieffer-Heeger model.*—We begin with a non-Hermitian one-dimensional topological insulator, the Su-Schrieffer-Heeger (SSH) model with non-reciprocal intracell hopping [57]. The Bloch Hamiltonian is given by

$$H_{\text{SSH}}(k) = \left( \frac{t_1 + t_2}{2} + t \cos k \right) \sigma_x + \left( i \frac{t_1 - t_2}{2} + t \sin k \right) \sigma_y, \quad (2)$$

where  $\sigma_i$  ( $i = x, y$ ) are the Pauli matrices,  $t \in \mathbb{R}$  is the intercell hopping, and  $t_1 \in \mathbb{C}$  and  $t_2 \in \mathbb{R}$  are the intracell directional hoppings. The Hamiltonian becomes Hermitian when  $t_1 = t_2$ . Considering the SSH model along the  $x$ -axis without loss of generality, the Berry curvature vanishes, and Eq. (1) simplifies to

$$\sigma_{xxx} = -e^3 \text{Re} \int_{\mathbf{k}} f_0 \left\{ \tau^2 \partial_x^3 \xi_{\mathbf{k}}^{(0)} + \partial_x G_{xx}^{LR(0)} \right\}. \quad (3)$$

The non-Hermitian SSH model preserves time-reversal symmetry, given by  $H_{\text{SSH}}(k)^* = H_{\text{SSH}}(-k)$  when  $t_1 \in$

$\mathbb{R}$ . Under this symmetry, the band dispersion satisfies  $\xi_{\mathbf{k}}^{(0)*} = \xi_{-\mathbf{k}}^{(0)}$ , and the Berry connection obeys  $A_{mn,\nu}^{LR(0)}(k)^* = A_{mn,\nu}^{LR(0)}(-k)$ , ensuring  $\sigma_{xxx} = 0$ . To obtain a nonzero  $\sigma_{xxx}$ , we introduce a complex  $t_1$ , which breaks time-reversal symmetry. The value of  $t_1$  is chosen to maintain a finite line gap [Fig. 1(a)].

As shown in Eq. (3), the real part of the band-renormalized QM provides an intrinsic contribution to the second-order DC conductivity (SODCc), which is independent of  $\tau$ . Its temperature dependence is shown in Fig. 1(b). The ratio of the intrinsic term  $\sigma_{xxx}^0$  to the total SODCc  $\sigma_{xxx}$  increases with  $T$ . In the strong scattering regime ( $\tau = 1$ ), the intrinsic term dominates the SODCc [Fig. 1(c)]. In contrast, in the weak scattering regime ( $\tau = 10$ ), the intrinsic contribution is small at low  $T$  but increases with temperature.

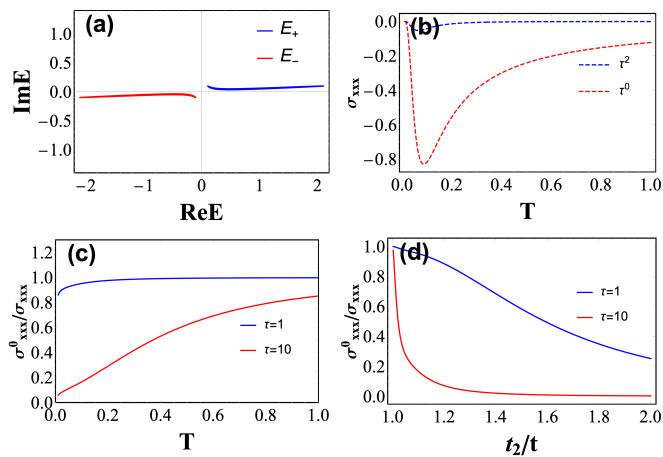


Fig. 1. SODCc in the non-Hermitian SSH model. (a) Band dispersion for  $t_2/t = 1.1$ . (b) Intrinsic contribution (order  $\tau^0$ ) and the coefficient of the  $\tau^2$  term in the SODCc. (c) Ratio of the intrinsic contribution to the total SODCc as a function of  $T$  for  $t_2/t = 1.1$ ; (d) the same ratio as a function of  $t_2/t$  for  $T = 0.1$ . Other parameters:  $t_1/t = t_2/t + i0.2$ .

The energy gap of the non-Hermitian SSH model closes at the critical point  $t_2/t = 1$ . Near this critical value, the intrinsic contribution dominates the SODCc in both the strong ( $\tau = 1$ ) and weak ( $\tau = 10$ ) scattering regimes [Fig. 1(d)].

*Boundary of a Chern insulator.*—Next, we consider a one-dimensional system that forms the boundary of a Chern insulator. Previous studies [58] have shown that the low-energy physics of this boundary can be effectively captured by a non-Hermitian Hamiltonian, where non-Hermiticity arises from the coupling between the boundary and the bulk, thereby inducing a complex self-energy. The

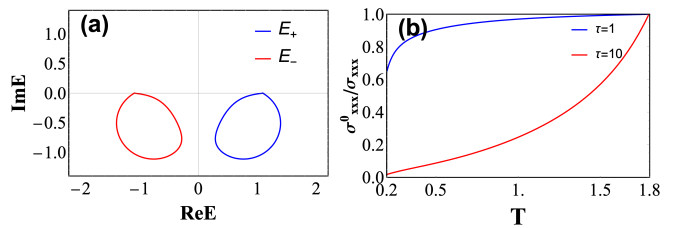


Fig. 2. SODCc at the boundary of a Chern insulator. (a) Band dispersion of the Hamiltonian in Eq. (4). (b) Ratio of the intrinsic contribution to the total SODCc as a function of temperature  $T$ . The parameters are  $m = -1.9$  and  $\eta = 1/\sqrt{80}$ .

effective non-Hermitian Hamiltonian takes the form

$$H_{edge}(k) = \left( \sin k - \frac{1 - (m + \cos k)^2}{2(i\eta - \sin k)} \right) \sigma_y + (m + \cos k) \sigma_z + \frac{1 - (m + \cos k)^2}{2(i\eta - \sin k)} \sigma_0. \quad (4)$$

Furthermore, the model exhibits a phase with a line gap (see Fig. 2(a)). As illustrated in Fig. 2(b), the intrinsic contribution to the total SODCc increases with temperature in both the strong and weak scattering regimes. Notably, at low temperatures, the intrinsic contribution is more pronounced in the strong scattering regime than in the weak scattering regime.

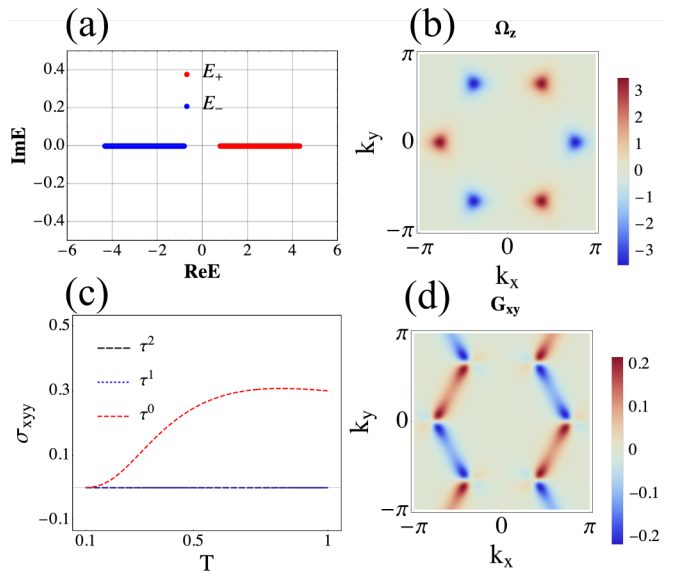


Fig. 3. Band dispersion (a), (c) SODCc  $\sigma_{xyy}$  as a function of  $T$ , and momentum-space distributions of the Berry curvature (b) and the  $xy$ -component of the QM,  $G_{xy}$  (d), for parameters  $m = 0.8$ ,  $\gamma = 0.5$ .

*Non-Hermitian two-dimensional model with real spectrum.*— We proceed to study the effect of the QGT on the SODCc in a 2D non-Hermitian model with a Hamiltonian

that reads [59]:

$$H_{2d}(k_x, k_y) = \begin{bmatrix} m & h(k_x, k_y) \\ \frac{1}{\gamma} h(k_x, k_y)^* & -m \end{bmatrix} \quad (5)$$

where the function  $h(k_x, k_y) = e^{-ik_y} + 2e^{ik_y/2} \cos\left(\frac{\sqrt{3}}{2}k_x\right)$  defines the system such that for  $\gamma \neq 1$  the Hamiltonian is non-Hermitian yet can exhibit real eigenvalues [Fig. 3(a)]. Both the Berry curvature and the QM are real-valued functions of the Bloch momentum  $\mathbf{k}$ ; accordingly, Figs. 3(b) and 3(d) display the distributions of the Berry curvature  $\Omega_z(k_x, k_y)$  and the QM component  $G_{xy}$  in  $\mathbf{k}$ -space.

Notably, the Berry curvature satisfies  $\Omega_z(k_x, k_y) = -\Omega_z(-k_x, k_y)$  and  $\Omega_z(k_x, k_y) = \Omega_z(k_x, -k_y)$ , while the QM component obeys  $G_{xy}(k_x, k_y) = -G_{xy}(-k_x, k_y)$  and  $G_{xy}(k_x, k_y) = -G_{xy}(k_x, -k_y)$ . Taking the  $xyy$ -component of the SODCc,  $\sigma_{xyy}$ , as a concrete example and noting that  $E_{\pm}(\mathbf{k}) = E_{\pm}(-\mathbf{k})$ , both the first- and second-order  $\tau$  terms in Eq. (3) vanish, so that only the band-renormalized QM, which is independent of  $\tau$ , contributes to  $\sigma_{xyy}$  [see Fig. 3(c)].

In non-Hermitian systems, the QGT exhibits a complex structure. While the QGT's imaginary part in Hermitian systems corresponds to the purely real Berry curvature, the Berry curvature in non-Hermitian systems becomes intrinsically complex. This complexity introduces an imaginary component to the curvature, which dynamically couples to the spatial width of quantum wavepackets within the semiclassical equations of motion  $\dot{\mathbf{k}} = -e\mathbf{E} + W^2 \text{Im}[\nabla_{\mathbf{k}} \xi_{n,\mathbf{k}} + e\mathbf{E} \times \Omega_{n,\mathbf{k}}]$ . The conventional narrow wavepacket approximation, however, suppresses this coupling by neglecting finite-width contributions. To address this limitation and elucidate the role of the non-Hermitian Berry curvature in material responses, we explicitly incorporate a finite wavepacket width and analyze its impact on the SODCc.

*Effect of Wavepacket Width on SODCc.* — Assuming the imaginary component of the band dispersion is perturbatively small compared to all other energy scales (e.g., real band energies and scattering rates), we derive the SODCc as (see Appendix A for details):

$$\sigma_{\mu\nu\theta}^W = \sigma_{\mu\nu\theta}^{W=0} + e^3 \int_{\mathbf{k}} W^2 \tau \Gamma_{2,1} + W^2 \tau^2 \Gamma_{2,2} + W^4 \tau^2 \Gamma_{4,2}, \quad (6)$$

The term  $\sigma_{\mu\nu\theta}^{W=0}$  represents the DC conductivity in the narrow wavepacket width limit, i.e., Eq. (1). The coefficients  $\Gamma_{2,1}$ ,  $\Gamma_{2,2}$ , and  $\Gamma_{4,2}$  encode the interplay between finite wavepacket width and the complex QGT. These

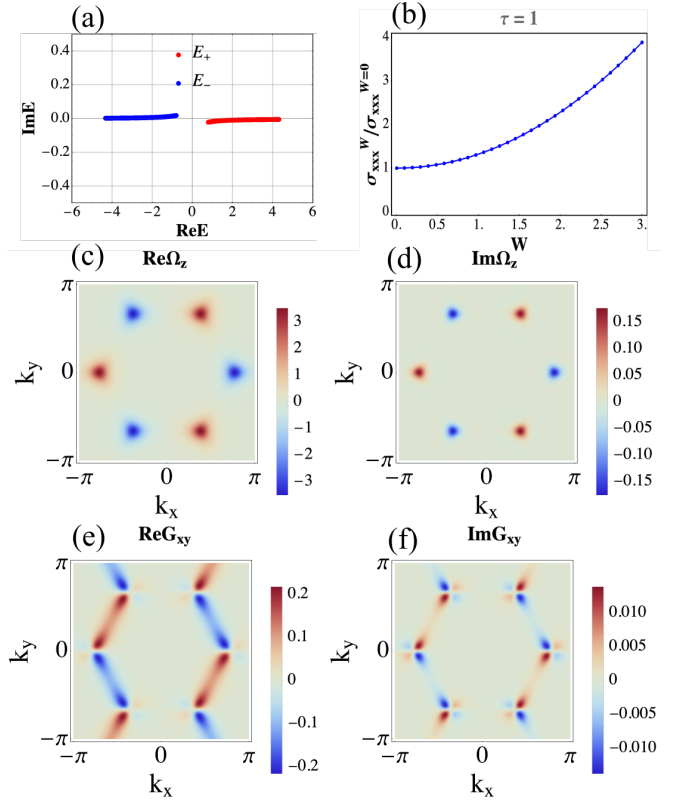


Fig. 4. Band dispersion (a), SODCc  $\sigma_{xxx}$  as a function of  $W$  (b), and momentum-space distributions of typical components of the QGT (c-f). Parameters:  $m = 0.8 - 0.02i$ ,  $\gamma = 0.5$ .

terms are defined as

$$\begin{aligned} \Gamma_{2,1} &= \left[ \frac{\epsilon_{i\nu l} \epsilon_{\mu\theta\gamma} \partial_i f_0 \text{Im}\Omega_l^{(0)} \text{Re}\Omega_\gamma^{(0)} + (\theta \leftrightarrow \nu)}{2} \right. \\ &\quad \left. + \frac{(2\partial_\theta \text{Im}G_{\nu i}^{LR} - \partial_i \text{Im}G_{\nu\theta}^{LR}) \partial_i f_0 + (\theta \leftrightarrow \nu)}{2} \right] \partial_\mu \text{Re}\xi_{\mathbf{k}}^{(0)}, \\ \Gamma_{2,2} &= \frac{1}{2} \left[ \epsilon_{j\theta i} \left( \partial_\nu \text{Im}\Omega_i^{(0)} \partial_j f_0 \right. \right. \\ &\quad \left. \left. + 2 \text{Im}\Omega_i^{(0)} \partial_j \partial_\nu f_0 \right) + (\theta \leftrightarrow \nu) \right] \partial_\mu \text{Re}\xi_{\mathbf{k}}^{(0)}, \\ \Gamma_{4,2} &= \frac{\epsilon_{i\nu j} \epsilon_{n\theta\gamma} \text{Im}\Omega_j \partial_i (\text{Im}\Omega_\gamma \partial_n f_0) + (\theta \leftrightarrow \nu)}{2} \partial_\mu \text{Re}\xi_{\mathbf{k}}^{(0)}. \end{aligned} \quad (7)$$

The coefficients  $\Gamma_{2,2}$  and  $\Gamma_{4,2}$  depend solely on the imaginary part of the non-Hermitian Berry curvature. In contrast, the coefficient  $\Gamma_{2,1}$  involves contributions from both the full complex non-Hermitian Berry curvature and the imaginary part of the non-Hermitian band-renormalized QM.

To elucidate the role of the wavepacket width in the SODCc, we introduce a small imaginary perturbation to the parameter  $m$  in the model defined by the Hamiltonian (5). This modification results in a Hamiltonian

with complex eigenvalues and a line gap [Fig. 4(a)], while the QM and Berry curvature acquire complex character, as illustrated in Figs. 4(c–f). Consequently, all coefficients  $\Gamma_{i,j}$  become non-zero, leading to a wavepacket-width-dependent enhancement of  $\sigma_{xxx}^W$ , as demonstrated in Fig. 4(b).

*Conclusions and Outlook.*— In this work, we reveal the role of the QGT in governing nonlinear electrical responses in non-Hermitian systems with a spectral line gap. In the narrow-wavepacket-width limit, the SODCc depends solely on the real part of the band dispersion, the Berry curvature, and the band-renormalized QM. Beyond this limit, the wavepacket width bridges the complex QM and Berry curvature—unique features of the projected Hilbert space in non-Hermitian systems—to the nonlinear response. Using 1D and 2D non-Hermitian models, we demonstrate the distinct role of the QM in shaping the SODCc. Notably, in the narrow-wavepacket regime, our results suggest that the band-renormalized QM governs the SODCc independently of the scattering rate. Furthermore, the wavepacket width amplifies the SODCc, a phenomenon unique to non-Hermitian systems arising from the imaginary components of the band dispersion and Berry curvature. These contributions introduce terms proportional to the wavepacket width that modify the semiclassical equations of motion.

Our results extend to surfaces and edges of topological materials, such as Chern insulators, which are effectively described by non-Hermitian Hamiltonians. This connection enables predictions of surface nonlinear conductivity in Hermitian systems. By bridging quantum geometry with nonlinear transport, this work establishes a framework to harness geometric effects in topological devices and engineered materials.

*Acknowledgments*— K.C. acknowledges support from the Fundamental Research Funds for the Central Universities. J.Z. acknowledges support from the National Natural Science Foundation of China (Grants No. 92263208), the National Key R&D Program of China (Grants No. 2022YFA1404400), and the Research Grants Council of Hong Kong SAR (Grant No. AoE/P-502/20).

$\times$ : KaiChenPhys@tongji.edu.cn  $^+$ : jiezhutongji.edu.cn

- 
- [1] J. Provost and G. Vaille, *Communications in Mathematical Physics* **76**, 289 (1980).  
 [2] M. Kolodrubetz, D. Sels, P. Mehta, and A. Polkovnikov, *Physics Reports* **697**, 1 (2017).  
 [3] E. Rossi, *Current Opinion in Solid State and Materials Science* **25**, 100952 (2021).  
 [4] M. V. Berry, *Proceedings of the Royal Society of London. A. Mathematical and Physical Sciences* **392**, 45 (1984).  
 [5] G. Fubini, *Sulle metriche definite da una forma hermitiana: nota* (Office graf. C. Ferrari, 1904).  
 [6] E. Study, *Mathematische Annalen* **60**, 321 (1905).  
 [7] C.-X. Liu, S.-C. Zhang, and X.-L. Qi, *Annual Review of Condensed Matter Physics* **7**, 301 (2016).  
 [8] C.-Z. Chang, C.-X. Liu, and A. H. MacDonald, *Reviews of Modern Physics* **95**, 011002 (2023).  
 [9] M. Z. Hasan and C. L. Kane, *Reviews of modern physics* **82**, 3045 (2010).  
 [10] X.-L. Qi and S.-C. Zhang, *Reviews of modern physics* **83**, 1057 (2011).  
 [11] S. M. Young, S. Zaheer, J. C. Teo, C. L. Kane, E. J. Mele, and A. M. Rappe, *Physical review letters* **108**, 140405 (2012).  
 [12] P. Hosur and X. Qi, *Comptes Rendus. Physique* **14**, 857 (2013).  
 [13] S. M. Young and C. L. Kane, *Physical review letters* **115**, 126803 (2015).  
 [14] B. Yan and C. Felser, *Annual Review of Condensed Matter Physics* **8**, 337 (2017).  
 [15] T. Thonhauser, D. Ceresoli, D. Vanderbilt, and R. Resta, *Physical review letters* **95**, 137205 (2005).  
 [16] R. Resta, *Journal of Physics: Condensed Matter* **22**, 123201 (2010).  
 [17] D. Xiao, M.-C. Chang, and Q. Niu, *Reviews of modern physics* **82**, 1959 (2010).  
 [18] K. Chen, S. Nanda, and P. Hosur, *Physical Review B* **110**, 195145 (2024).  
 [19] R. Roy, *Physical Review B* **90**, 165139 (2014).  
 [20] K. Kim, A. DaSilva, S. Huang, B. Fallahazad, S. Larentis, T. Taniguchi, K. Watanabe, B. J. LeRoy, A. H. MacDonald, and E. Tutuc, *Proceedings of the National Academy of Sciences* **114**, 3364 (2017).  
 [21] Y. Cao, V. Fatemi, A. Demir, S. Fang, S. L. Tomarken, J. Y. Luo, J. D. Sanchez-Yamagishi, K. Watanabe, T. Taniguchi, E. Kaxiras, *et al.*, *Nature* **556**, 80 (2018).  
 [22] Y. Cao, V. Fatemi, S. Fang, K. Watanabe, T. Taniguchi, E. Kaxiras, and P. Jarillo-Herrero, *Nature* **556**, 43 (2018).  
 [23] M. Yankowitz, S. Chen, H. Polshyn, Y. Zhang, K. Watanabe, T. Taniguchi, D. Graf, A. F. Young, and C. R. Dean, *Science* **363**, 1059 (2019).  
 [24] G. Chen, A. L. Sharpe, P. Gallagher, I. T. Rosen, E. J. Fox, L. Jiang, B. Lyu, H. Li, K. Watanabe, T. Taniguchi, *et al.*, *Nature* **572**, 215 (2019).  
 [25] X. Lu, P. Stepanov, W. Yang, M. Xie, M. A. Aamir, I. Das, C. Urgell, K. Watanabe, T. Taniguchi, G. Zhang, *et al.*, *Nature* **574**, 653 (2019).  
 [26] S. Peotta and P. Törmä, *Nature communications* **6**, 8944 (2015).  
 [27] F. Xie, Z. Song, B. Lian, and B. A. Bernevig, *Physical review letters* **124**, 167002 (2020).  
 [28] L. Liang, T. I. Vanhala, S. Peotta, T. Siro, A. Harju, and P. Törmä, *Physical Review B* **95**, 024515 (2017).  
 [29] V. Peri, Z.-D. Song, B. A. Bernevig, and S. D. Huber, *Physical review letters* **126**, 027002 (2021).  
 [30] K. Chen, B. Karki, and P. Hosur, *arXiv preprint arXiv:2501.16965* (2025).  
 [31] B. Ghosh, Y. Onishi, S.-Y. Xu, H. Lin, L. Fu, and A. Bansil, *Science Advances* **10**, eado1761 (2024).  
 [32] M. Ezawa, *Physical Review B* **110**, 195437 (2024).  
 [33] M. Ezawa, *Physical Review B* **110**, L241405 (2024).  
 [34] K. Das, S. Lahiri, R. B. Atencia, D. Culcer, and A. Agarwal, *Physical Review B* **108**, L201405 (2023).  
 [35] N. Wang, D. Kaplan, Z. Zhang, T. Holder, N. Cao, A. Wang, X. Zhou, F. Zhou, Z. Jiang, C. Zhang, *et al.*, *Nature* **621**, 487 (2023).  
 [36] Y. Fang, J. Cano, and S. A. A. Ghorashi, *Physical Review*

- Letters **133**, 106701 (2024).
- [37] D. Mandal, S. Sarkar, K. Das, and A. Agarwal, Physical Review B **110**, 195131 (2024).
- [38] K. Das, K. Ghorai, D. Culcer, and A. Agarwal, Physical review letters **132**, 096302 (2024).
- [39] C. M. Bender, Reports on Progress in Physics **70**, 947 (2007).
- [40] R. El-Ganainy, K. G. Makris, M. Khajavikhan, Z. H. Musslimani, S. Rotter, and D. N. Christodoulides, Nature Physics **14**, 11 (2018).
- [41] E. J. Bergholtz, J. C. Budich, and F. K. Kunst, Reviews of Modern Physics **93**, 015005 (2021).
- [42] X. Zhang, T. Zhang, M.-H. Lu, and Y.-F. Chen, Advances in Physics: X **7**, 2109431 (2022).
- [43] K. Ding, C. Fang, and G. Ma, Nature Reviews Physics **4**, 745 (2022).
- [44] K. Kawabata, T. Bessho, and M. Sato, Physical review letters **123**, 066405 (2019).
- [45] L. Pan, X. Chen, Y. Chen, and H. Zhai, Nature Physics **16**, 767 (2020).
- [46] D. Sticlet, B. Dóra, and C. P. Moca, Physical Review Letters **128**, 016802 (2022).
- [47] J.-H. Wang, Y.-L. Tao, and Y. Xu, Chinese Physics Letters **39**, 010301 (2022).
- [48] K. Kawabata, K. Shiozaki, M. Ueda, and M. Sato, Physical Review X **9**, 041015 (2019).
- [49] K. Chen and A. B. Khanikaev, Physical Review B **105**, L081112 (2022).
- [50] A. Altland and M. R. Zirnbauer, Physical Review B **55**, 1142 (1997).
- [51] H. Zhou and J. Y. Lee, Physical Review B **99**, 235112 (2019).
- [52] N. Okuma and M. Sato, Annual Review of Condensed Matter Physics **14**, 83 (2023).
- [53] Y. Ashida, Z. Gong, and M. Ueda, Advances in Physics **69**, 249 (2020).
- [54] F. Schindler, K. Gu, B. Lian, and K. Kawabata, PRX Quantum **4**, 030315 (2023).
- [55] W. Dong, Q.-D. Jiang, and M. Baggioli, arXiv preprint arXiv:2501.12163 (2025).
- [56] D. Kaplan, T. Holder, and B. Yan, Physical review letters **132**, 026301 (2024).
- [57] C. Chen Ye, W. Vleeshouwers, S. Heatley, V. Gritsev, and C. Morais Smith, Physical Review Research **6**, 023202 (2024).
- [58] S. Hamanaka, T. Yoshida, and K. Kawabata, arXiv preprint arXiv:2405.10015 (2024).
- [59] Y. Long, H. Xue, and B. Zhang, Physical Review B **105**, L100102 (2022).

### Appendix A: Nonlinear electric response and the quantum geometric tensor

In this section, we derive the nonlinear electric response of a non-Hermitian system under an external electric field and reveal its connection to the quantum geometric tensor associated with the system. Starting from the semiclassical equation of motion [55]:

$$\begin{cases} \dot{\mathbf{r}} = \text{Re} [\nabla_{\mathbf{k}} \xi_{n,\mathbf{k}} + e\mathbf{E} \times \boldsymbol{\Omega}_{n,\mathbf{k}}], \\ \dot{\mathbf{k}} = -e\mathbf{E} + W^2 \text{Im} [\nabla_{\mathbf{k}} \xi_{n,\mathbf{k}} + e\mathbf{E} \times \boldsymbol{\Omega}_{n,\mathbf{k}}] \equiv \mathbf{W}_{\mathbf{k}}. \end{cases} \quad (\text{A1})$$

where  $\mathbf{E}$  is the external electric field,  $W$  is the width of the Gaussian wavepacket, and  $\xi_{n,\mathbf{k}}$  and  $\boldsymbol{\Omega}_{n,\mathbf{k}} \equiv i\nabla_{\mathbf{k}} \times \langle \psi_{n,\mathbf{k}}^L | \nabla_{\mathbf{k}} \psi_{n,\mathbf{k}}^R \rangle$  denote the  $n$ th band energy and the Berry curvature, respectively.

In this work, we focus on a nondegenerate band and, to simplify the notation when there is no risk of confusion, omit the target band index. Under the relaxation time approximation [47] and assuming a spatially uniform distribution function  $f$ , the Boltzmann equation for the electron distribution is given by:

$$\partial_t f + \dot{\mathbf{k}} \cdot \nabla_{\mathbf{k}} f = -\frac{f - f_0}{\tau}, \quad (\text{A2})$$

where  $\tau$  is the scattering time and  $f_0$  is the equilibrium distribution function in the absence of external fields. In a non-Hermitian system, for the target band, we have

$$f_0 = \frac{1}{1 + \exp(\text{Re} \xi_{\mathbf{k}}/k_B T)},$$

with the Boltzmann constant  $k_B$  set to 1 throughout this work.

The electron current is given by:

$$\mathbf{J} = -e \int_{\mathbf{k}} f \dot{\mathbf{r}} = -e \int_{\mathbf{k}} f \mathbf{v}. \quad (\text{A3})$$

The higher-order response is extracted via the Schrieffer-Wolff transformation, as demonstrated in Refs. [36, 56] for Hermitian systems. In the weak-field limit, we expand the distribution function  $f$ , the group velocity  $\mathbf{v}$ , the band dispersion  $\xi_{\mathbf{k}}$ , and the Berry curvature  $\boldsymbol{\Omega}_{\mathbf{k}}$  in powers of the external field  $\mathbf{E}$  as follows:

$$\left\{ \begin{array}{l} f = \sum_{n=0} f^{(n)}, \mathbf{v} = \sum_{n=0} \mathbf{v}^{(n)}, \\ \xi_{\mathbf{k}} = \sum_{n=0} \xi_{\mathbf{k}}^{(n)}, \Omega_{\mathbf{k}} = \sum_{n=0} \Omega_{\mathbf{k}}^{(n)}, \\ \mathbf{W}_{\mathbf{k}} = \sum_{n=0} \mathbf{W}_{\mathbf{k}}^{(n)}, \mathbf{J} = \sum_{n=0} \mathbf{J}_{\mathbf{k}}^{(n)}. \end{array} \right. \quad (\text{A4})$$

From the first equation in Eqs. (A1), the three lowest-order terms in the expansion of the group velocity are given by:

$$\left\{ \begin{array}{l} \mathbf{v}^{(0)} = \text{Re} \nabla_{\mathbf{k}} \xi_{\mathbf{k}}^{(0)}, \\ \mathbf{v}^{(1)} = \text{Re} \left[ \nabla_{\mathbf{k}} \xi_{\mathbf{k}}^{(1)} + e\mathbf{E} \times \Omega_{\mathbf{k}}^{(0)} \right], \\ \mathbf{v}^{(2)} = \text{Re} \left[ \nabla_{\mathbf{k}} \xi_{\mathbf{k}}^{(2)} + e\mathbf{E} \times \Omega_{\mathbf{k}}^{(1)} \right], \\ \dots \end{array} \right. \quad (\text{A5})$$

Using the ansatz  $f = f e^{i\omega t}$  and the second equation in Eqs. (A1), Eq. (A2) becomes

$$i\omega f + \mathbf{W}_{\mathbf{k}} \cdot \nabla_{\mathbf{k}} f = -\frac{f - f_0}{\tau} \quad (\text{A6})$$

Substituting Eqs. (A4) into the above equation, we obtain:

$$\sum_{n=0} i\omega f^{(n)} + \sum_{i,j=0} \mathbf{W}_{\mathbf{k}}^{(i)} \cdot \nabla_{\mathbf{k}} f^{(j)} = \frac{f_0 - f^{(0)}}{\tau} - \sum_{l=1} \frac{f^{(l)}}{\tau} \quad (\text{A7})$$

Then  $f^{(n)}$  can be obtained recursively as:

$$\left\{ \begin{array}{l} i\omega f^{(0)} + \mathbf{W}_{\mathbf{k}}^{(0)} \cdot \nabla_{\mathbf{k}} f^{(0)} = \frac{f_0 - f^{(0)}}{\tau}, \\ i\omega f^{(1)} + \mathbf{W}_{\mathbf{k}}^{(0)} \cdot \nabla_{\mathbf{k}} f^{(1)} + \mathbf{W}_{\mathbf{k}}^{(1)} \cdot \nabla_{\mathbf{k}} f^{(0)} = -\frac{f^{(1)}}{\tau}, \\ i\omega f^{(2)} + \mathbf{W}_{\mathbf{k}}^{(0)} \cdot \nabla_{\mathbf{k}} f^{(2)} + \mathbf{W}_{\mathbf{k}}^{(2)} \cdot \nabla_{\mathbf{k}} f^{(0)} + \mathbf{W}_{\mathbf{k}}^{(1)} \cdot \nabla_{\mathbf{k}} f^{(1)} = -\frac{f^{(2)}}{\tau}, \\ \dots \end{array} \right. \quad (\text{A8})$$

where  $\mathbf{W}_{\mathbf{k}}^{(0)} = W^2 \nabla_{\mathbf{k}} \text{Im} \xi_{\mathbf{k}}^{(0)}$ ,  $\mathbf{W}_{\mathbf{k}}^{(1)} = -e\mathbf{E} + W^2 \text{Im} \left[ \nabla_{\mathbf{k}} \xi_{\mathbf{k}}^{(1)} + e\mathbf{E} \times \Omega_{\mathbf{k}}^{(0)} \right]$  and  $\mathbf{W}_{\mathbf{k}}^{(2)} = W^2 \text{Im} \left[ \nabla_{\mathbf{k}} \xi_{\mathbf{k}}^{(2)} + e\mathbf{E} \times \Omega_{\mathbf{k}}^{(1)} \right]$ . In the direct current limit, where  $\omega \ll 1/\tau$ , the above equations simplify to:

$$\left\{ \begin{array}{l} \mathbf{W}_{\mathbf{k}}^{(0)} \cdot \nabla_{\mathbf{k}} f^{(0)} = \frac{f_0 - f^{(0)}}{\tau}, \\ \mathbf{W}_{\mathbf{k}}^{(0)} \cdot \nabla_{\mathbf{k}} f^{(1)} + \mathbf{W}_{\mathbf{k}}^{(1)} \cdot \nabla_{\mathbf{k}} f^{(0)} = -\frac{f^{(1)}}{\tau}, \\ \mathbf{W}_{\mathbf{k}}^{(0)} \cdot \nabla_{\mathbf{k}} f^{(2)} + \mathbf{W}_{\mathbf{k}}^{(2)} \cdot \nabla_{\mathbf{k}} f^{(0)} + \mathbf{W}_{\mathbf{k}}^{(1)} \cdot \nabla_{\mathbf{k}} f^{(1)} = -\frac{f^{(2)}}{\tau}, \\ \dots \end{array} \right. \quad (\text{A9})$$

Substituting the solutions for  $f^{(n)}$  and those from Eqs. (A5) into Eq. (A3) yields, in principle, the electrical response to any order.

### 1. narrow wave packet width

In this subsection, we consider the limit of a narrow wave packet width, such that the term proportional to  $W^2$  in  $\mathbf{W}_{\mathbf{k}}$  can be safely neglected. We then obtain:

$$\begin{cases} f^{(0)} = f_0, \\ f^{(1)} = \tau e \mathbf{E} \cdot \nabla_{\mathbf{k}} f^{(0)}, \\ f^{(2)} = \tau e \mathbf{E} \cdot \nabla_{\mathbf{k}} f^{(1)}, \\ \dots \end{cases} \quad (\text{A10})$$

The currents to first and second order in the electric field are given by:

$$\begin{cases} \mathbf{J}^{(1)} = -e \int_{\mathbf{k}} f^{(1)} \text{Re} \nabla_{\mathbf{k}} \xi_{\mathbf{k}}^{(0)} + f^{(0)} \text{Re} \left[ \nabla_{\mathbf{k}} \xi_{\mathbf{k}}^{(1)} + e \mathbf{E} \times \boldsymbol{\Omega}_{\mathbf{k}}^{(0)} \right], \\ = -e \int_{\mathbf{k}} \tau e \mathbf{E} \cdot \nabla_{\mathbf{k}} f^{(0)} \text{Re} \nabla_{\mathbf{k}} \xi_{\mathbf{k}}^{(0)} + f^{(0)} \text{Re} \left[ \nabla_{\mathbf{k}} \xi_{\mathbf{k}}^{(1)} + e \mathbf{E} \times \boldsymbol{\Omega}_{\mathbf{k}}^{(0)} \right], \end{cases} \quad (\text{A11})$$

and

$$\mathbf{J}^{(2)} = -e \int_{\mathbf{k}} f^{(0)} \text{Re} \left[ \nabla_{\mathbf{k}} \xi_{\mathbf{k}}^{(2)} + e \mathbf{E} \times \boldsymbol{\Omega}_{\mathbf{k}}^{(1)} \right] + f^{(1)} \text{Re} \left[ \nabla_{\mathbf{k}} \xi_{\mathbf{k}}^{(1)} + e \mathbf{E} \times \boldsymbol{\Omega}_{\mathbf{k}}^{(0)} \right] + f^{(2)} \text{Re} \nabla_{\mathbf{k}} \xi_{\mathbf{k}}^{(0)} \quad (\text{A12})$$

To analyze the corrections to the band dispersion and Berry curvature induced by an external field  $\mathbf{E}$ , we expand  $\xi_{\mathbf{k}}$  and  $\boldsymbol{\Omega}_{\mathbf{k}}$  up to third order in  $\mathbf{E}$ . In the presence of the external field, the system Hamiltonian takes the form

$$H_{NH} = \sum_{m,n} \left( \xi_{n,\mathbf{k}}^{(0)} \delta_{mn} - e \langle \psi_{m,\mathbf{k}}^L | \mathbf{E} \cdot \mathbf{r} | \psi_{n,\mathbf{k}}^R \rangle \right) | \psi_{m,\mathbf{k}}^R \rangle \langle \psi_{n,\mathbf{k}}^L | \equiv H_0 + H_1 \quad (\text{A13})$$

with

$$\begin{cases} H_0 = \sum_n \left( \xi_{n,\mathbf{k}}^{(0)} - e \mathbf{E} \cdot \mathbf{A}_{nn}^{LR} \right) | \psi_{n,\mathbf{k}}^R \rangle \langle \psi_{n,\mathbf{k}}^L |, \\ H_1 = \sum_{m \neq n} -e \mathbf{E} \cdot \mathbf{A}_{mn}^{LR} | \psi_{m,\mathbf{k}}^R \rangle \langle \psi_{n,\mathbf{k}}^L |, \end{cases} \quad (\text{A14})$$

where  $\mathbf{A}_{mn}^{LR} \equiv i \langle \psi_{m,\mathbf{k}}^L | \nabla_{\mathbf{k}} \psi_{n,\mathbf{k}}^R \rangle$ . The Schrieffer-Wolff operator  $S$  perturbs an operator  $O$ , yielding a transformed operator  $O' = e^S O e^{-S}$ .

The operator  $S$  is chosen to satisfy  $H_1 + [S, H_0] = 0$  which leads to

$$\sum_{m \neq n} e \mathbf{E} \cdot \mathbf{A}_{mn}^{LR} | \psi_{m,\mathbf{k}}^R \rangle \langle \psi_{n,\mathbf{k}}^L | = \sum_{i,j} S_{ij} | \psi_{i,\mathbf{k}}^R \rangle \langle \psi_{j,\mathbf{k}}^L | \left[ \left( \xi_{j,\mathbf{k}}^{(0)} - e \mathbf{E} \cdot \mathbf{A}_{jj}^{LR} \right) - \left( \xi_{i,\mathbf{k}}^{(0)} - e \mathbf{E} \cdot \mathbf{A}_{ii}^{LR} \right) \right], \quad (\text{A15})$$

we have:

$$\begin{cases} S_{nn} = 0, \\ S_{m \neq n} = \frac{e \mathbf{E} \cdot \mathbf{A}_{mn}^{LR}}{\left( \xi_{n,\mathbf{k}}^{(0)} - e \mathbf{E} \cdot \mathbf{A}_{nn}^{LR} \right) - \left( \xi_{m,\mathbf{k}}^{(0)} - e \mathbf{E} \cdot \mathbf{A}_{mm}^{LR} \right)} \approx \frac{e \mathbf{E} \cdot \mathbf{A}_{mn}^{LR}}{\left( \xi_{n,\mathbf{k}}^{(0)} - \xi_{m,\mathbf{k}}^{(0)} \right)} + \frac{e \mathbf{E} \cdot \mathbf{A}_{mn}^{LR} (e \mathbf{E} \cdot \mathbf{A}_{nn}^{LR} - e \mathbf{E} \cdot \mathbf{A}_{mm}^{LR})}{\left( \xi_{n,\mathbf{k}}^{(0)} - \xi_{m,\mathbf{k}}^{(0)} \right)^2} + O(E^3). \end{cases} \quad (\text{A16})$$

where, in the second equation, we use the fact that there exists a gap between the target band and the remaining bands.

The Hamiltonian is transform to

$$H'_{NH} = e^S H_{NH} e^{-S} = H_0 + \frac{[S, H_1]}{2} + \frac{[S, [S, H_1]]}{3} + \dots, \quad (\text{A17})$$

where

$$\frac{[S, H_1]}{2} = \frac{-e}{2} \sum_{m,n} \left( \sum_{i \neq n} S_{mi} \mathbf{E} \cdot \mathbf{A}_{in}^{LR} - \sum_{i \neq m} \mathbf{E} \cdot \mathbf{A}_{mi}^{LR} S_{in} \right) | \psi_{m,\mathbf{k}}^R \rangle \langle \psi_{n,\mathbf{k}}^L | \equiv \frac{-e}{2} \sum_{m,n} F_{mn} | \psi_{m,\mathbf{k}}^R \rangle \langle \psi_{n,\mathbf{k}}^L |, \quad (\text{A18})$$

and

$$\frac{[S, [S, H_1]]}{3} = O(E^3) \quad (\text{A19})$$

Now, the perturbed band dispersion  $\xi_{n,\mathbf{k}} = \langle \psi_{n,\mathbf{k}}^L | H' | \psi_{n,\mathbf{k}}^R \rangle$ , up to second order in the electric field, is given by:

$$\begin{cases} \xi_{n,\mathbf{k}}^{(1)} = -e \mathbf{E} \cdot \mathbf{A}_{nn}^{LR} = 0, \\ \xi_{n,\mathbf{k}}^{(2)} = \frac{-e^2}{2} \left( \sum_{m \neq n} \frac{\mathbf{E} \cdot \mathbf{A}_{mn}^{LR} \mathbf{E} \cdot \mathbf{A}_{nm}^{LR} + \mathbf{E} \cdot \mathbf{A}_{nm}^{LR} \mathbf{E} \cdot \mathbf{A}_{mn}^{LR}}{(\xi_{m,\mathbf{k}}^{(0)} - \xi_{n,\mathbf{k}}^{(0)})} \right) \equiv e^2 \sum_{\mu,\nu} G_{n,\mu\nu}^{LR} E^\mu E^\nu. \end{cases} \quad (\text{A20})$$

where, in the first equation, we choose a gauge for the Berry curvature to make it perpendicular to the electric field. Here,  $G_{n,\mu\nu}^{LR} = \sum_{i \neq n} \frac{A_{ni,\mu}^{LR} A_{in,\nu}^{LR} + A_{ni,\nu}^{LR} A_{in,\mu}^{LR}}{2(\xi_{n,\mathbf{k}}^{(0)} - \xi_{i,\mathbf{k}}^{(0)})}$  denotes the band-renormalized non-Hermitian quantum metric.

Similarly, the Berry connection  $\mathbf{A}^{LR} = \sum_{m,n} \mathbf{A}_{mn}^{LR} | \psi_{m,\mathbf{k}}^R \rangle \langle \psi_{n,\mathbf{k}}^L |$  transforms to:

$$\mathbf{A}'^{LR} = \sum_{m,n} \mathbf{A}_{mn}^{LR} | \psi_{m,\mathbf{k}}^R \rangle \langle \psi_{n,\mathbf{k}}^L | + \sum_{m,n} \left( \sum_{j \neq m} \frac{e \mathbf{E} \cdot \mathbf{A}_{mj}^{LR} \mathbf{A}_{jn}^{LR}}{(\xi_{j,\mathbf{k}}^{(0)} - \xi_{m,\mathbf{k}}^{(0)})} - \sum_{j \neq n} \frac{e \mathbf{A}_{mj}^{LR} \mathbf{E} \cdot \mathbf{A}_{jn}^{LR}}{(\xi_{n,\mathbf{k}}^{(0)} - \xi_{j,\mathbf{k}}^{(0)})} \right) | \psi_{m,\mathbf{k}}^R \rangle \langle \psi_{n,\mathbf{k}}^L | + O(E^2) \quad (\text{A21})$$

Therefore, the perturbed Berry connection for the  $n$ th band is given by:

$$\mathbf{A}_n^{(1)LR} = -e \sum_{j \neq n} \frac{\mathbf{E} \cdot \mathbf{A}_{nj}^{LR} \mathbf{A}_{jn}^{LR} + \mathbf{A}_{nj}^{LR} \mathbf{E} \cdot \mathbf{A}_{jn}^{LR}}{(\xi_{n,\mathbf{k}}^{(0)} - \xi_{j,\mathbf{k}}^{(0)})} = -e 2 G_{n,\mu\nu}^{LR} E^\mu \hat{x}_\nu, \quad (\text{A22})$$

where  $\hat{x}_\nu$  denotes the unit vector in the  $\nu$  direction, and the corresponding Berry curvature is:

$$\Omega_{n,\alpha}^{(1)LR} = -2e \epsilon_{\alpha\beta\nu} \partial_\beta G_{n,\mu\nu}^{LR} E^\mu, \quad (\text{A23})$$

Combining the above results, we can express the response current up to second order in the electric field, as shown below:

$$\begin{cases} \mathbf{J}^{(1)} = - \int_{\mathbf{k}} \tau e^2 \mathbf{E} \cdot \nabla_{\mathbf{k}} f^{(0)} \text{Re} \nabla_{\mathbf{k}} \xi_{\mathbf{k}}^{(0)} + f^{(0)} \text{Re} \left[ e^2 \mathbf{E} \times \Omega_{\mathbf{k}}^{(0)} \right], \\ J_i^{(1)} = -E^j \int_{\mathbf{k}} \tau e^2 \partial_j f_0 \partial_i \text{Re} \xi_{\mathbf{k}}^{(0)} + e^2 f_0 \epsilon_{ijl} \text{Re} \Omega_l^{(0)} = E^j \sigma_{ij}, \end{cases} \quad (\text{A24})$$

and

$$\begin{cases} \mathbf{J}^{(2)} = -e \int_{\mathbf{k}} f^{(0)} \text{Re} \left[ \nabla_{\mathbf{k}} \xi_{\mathbf{k}}^{(2)} + e \mathbf{E} \times \Omega_{\mathbf{k}}^{(1)} \right] + f^{(1)} \text{Re} \left[ e \mathbf{E} \times \Omega_{\mathbf{k}}^{(0)} \right] + f^{(2)} \text{Re} \nabla_{\mathbf{k}} \xi_{\mathbf{k}}^{(0)}, \\ J_i^{(2)} = -e \int_{\mathbf{k}} f_0 \text{Re} \left[ \partial_i \xi_{\mathbf{k}}^{(2)} + e \epsilon_{ijl} E^j \Omega_l^{(1)} \right] + f^{(1)} \text{Re} \left[ e \epsilon_{ijl} E^j \Omega_l^{(0)} \right] + f^{(2)} \text{Re} \partial_i \xi_{\mathbf{k}}^{(0)} = \sigma_{ijl} E^j E^l. \end{cases} \quad (\text{A25})$$

where

$$\begin{cases} f^{(0)} = f_0 = \frac{1}{1 + \exp^{\text{Re} \xi_{\mathbf{k}} / k_B T}}, \\ f^{(1)} = \tau e \mathbf{E} \cdot \nabla_{\mathbf{k}} f^{(0)} = e \tau E^j \partial_j f_0, \\ f^{(2)} = \tau e \mathbf{E} \cdot \nabla_{\mathbf{k}} f^{(1)} = (e \tau)^2 E^i E^j \partial_i \partial_j f_0, \\ \Omega_{\alpha}^{(1)} = -2e \epsilon_{\alpha\beta\nu} \partial_\beta G_{\mu\nu}^{LR} E^\mu, \\ \xi_{\mathbf{k}}^{(2)} = e^2 G_{\mu\nu}^{LR} E^\mu E^\nu \end{cases} \quad (\text{A26})$$

$$\left\{ \begin{aligned} \sigma_{i\mu\nu} &= \frac{\partial^2 J_i^{(2)}}{2\partial E^\mu \partial E^\nu} = -e^3 \int_{\mathbf{k}} \left\{ \tau^2 \partial_\mu \partial_\nu f_0 \text{Re} \left( \partial_i \xi_{\mathbf{k}}^{(0)} \right) - \tau f_0 \frac{\epsilon_{i\mu l} \partial_\nu \text{Re} \Omega_l^{(0)} + \epsilon_{i\nu l} \partial_\mu \text{Re} \Omega_l^{(0)}}{2} + f_0 \text{Re} \left[ 2\partial_i G_{\mu\nu}^{LR} - \frac{\partial_\nu G_{\mu i}^{LR} + \partial_\mu G_{\nu i}^{LR}}{2} \right] \right\}, \\ &= \sigma_{i\nu\mu} \end{aligned} \right. \quad (\text{A27})$$

Note that  $G_{\mu\nu}^{LR} = G_{\nu\mu}^{LR}$ .

## 2. Effects of Wave Packet Width

In the previous subsection, we considered the limit of a narrow wave packet, where the time evolution of momentum is solely dictated by the external electric field. However, in this limit, certain non-Hermitian effects are suppressed. Here, we extend our analysis to finite wave packet widths and examine their impact on the DC conductivity in non-Hermitian systems. To facilitate analytical progress, we focus on a non-Hermitian model in which the imaginary part of the spectrum varies slightly in  $\mathbf{k}$ -space within certain parameter regimes. In this case, the semiclassical equations of motion are modified as follows:

$$\left\{ \begin{aligned} \dot{\mathbf{r}} &= \text{Re} [\nabla_{\mathbf{k}} \xi_{n,\mathbf{k}} + e\mathbf{E} \times \boldsymbol{\Omega}_{n,\mathbf{k}}], \\ \dot{\mathbf{k}} &= -e\mathbf{E} + W^2 \text{Im} [e\mathbf{E} \times \boldsymbol{\Omega}_{n,\mathbf{k}}]. \end{aligned} \right. \quad (\text{A28})$$

Here,  $W$  denotes the wave-packet width. The distribution is modified as follows:

$$\left\{ \begin{aligned} f^{(0)} &= f_0, \\ f^{(1)} &= \tau e \left[ \mathbf{E} - W^2 \mathbf{E} \times \text{Im} \boldsymbol{\Omega}_{\mathbf{k}}^{(0)} \right] \cdot \nabla_{\mathbf{k}} f^{(0)}, \\ f^{(2)} &= \tau e \left[ \mathbf{E} - W^2 \mathbf{E} \times \text{Im} \boldsymbol{\Omega}_{\mathbf{k}}^{(0)} \right] \cdot \nabla_{\mathbf{k}} f^{(1)} - \tau W_{\mathbf{k}}^{(2)} \cdot \nabla_{\mathbf{k}} f^{(0)} \\ &= \tau e \left[ \mathbf{E} - W^2 \mathbf{E} \times \text{Im} \boldsymbol{\Omega}_{\mathbf{k}}^{(0)} \right] \cdot \nabla_{\mathbf{k}} f^{(1)} - \tau W^2 \text{Im} \left[ \nabla_{\mathbf{k}} \xi_{\mathbf{k}}^{(2)} + e\mathbf{E} \times \boldsymbol{\Omega}_{\mathbf{k}}^{(1)} \right] \cdot \nabla_{\mathbf{k}} f^{(0)}, \\ &\dots \end{aligned} \right. \quad (\text{A29})$$

where  $\xi_{\mathbf{k}}^{(2)} = e^2 \sum_{\mu,\nu} G_{\mu\nu}^{LR} E^\mu E^\nu$  and  $\Omega_{\alpha}^{(1)} = -2e\epsilon_{\alpha\beta\nu} \partial_\beta G_{\mu\nu}^{LR} E^\mu$ .

$$\left\{ \begin{aligned} \mathbf{J}^{(1)} &= -e \int_{\mathbf{k}} f^{(1)} \text{Re} \nabla_{\mathbf{k}} \xi_{\mathbf{k}}^{(0)} + f^{(0)} \text{Re} \left[ \nabla_{\mathbf{k}} \xi_{\mathbf{k}}^{(1)} + e\mathbf{E} \times \boldsymbol{\Omega}_{\mathbf{k}}^{(0)} \right], \\ &= -e \int_{\mathbf{k}} \tau e \mathbf{E} \cdot \nabla_{\mathbf{k}} f^{(0)} \text{Re} \nabla_{\mathbf{k}} \xi_{\mathbf{k}}^{(0)} + f^{(0)} e \mathbf{E} \times \text{Re} \boldsymbol{\Omega}_{\mathbf{k}}^{(0)} - \tau e \left[ W^2 \left( \mathbf{E} \times \text{Im} \boldsymbol{\Omega}_{\mathbf{k}}^{(0)} \right) \cdot \nabla_{\mathbf{k}} f^{(0)} \right] \text{Re} \nabla_{\mathbf{k}} \xi_{\mathbf{k}}^{(0)}, \\ &= \mathbf{J}^{(1)} (W=0) + \tau e^2 W^2 \int_{\mathbf{k}} \left[ \left( \mathbf{E} \times \text{Im} \boldsymbol{\Omega}_{\mathbf{k}}^{(0)} \right) \cdot \nabla_{\mathbf{k}} f^{(0)} \right] \text{Re} \nabla_{\mathbf{k}} \xi_{\mathbf{k}}^{(0)}, \end{aligned} \right. \quad (\text{A30})$$

the linear DC conductivity is now expressed as:

$$\sigma_{\mu\nu} = \sigma_{\mu\nu} (W=0) + \tau e^2 W^2 \int_{\mathbf{k}} \epsilon_{i\nu j} \text{Im} \Omega_j^{(0)} \partial_i f_0 \partial_\mu \text{Re} \xi_{\mathbf{k}}^{(0)} \quad (\text{A31})$$

and where  $\xi_{\mathbf{k}}^{(2)} = e^2 \sum_{\mu,\nu} G_{\mu\nu}^{LR} E^\mu E^\nu$  and  $\Omega_{\alpha}^{(1)} = -2e\epsilon_{\alpha\beta\nu} \partial_\beta G_{\mu\nu}^{LR} E^\mu$ .

$$\left\{ \begin{aligned} \mathbf{J}^{(2)} &= \mathbf{J}^{(2)} (W=0) + \tau W^2 e^3 \int_{\mathbf{k}} \text{Im} \left[ \mathbf{E} \times \boldsymbol{\Omega}_{\mathbf{k}}^{(0)} \right] \cdot \nabla_{\mathbf{k}} f_0 \text{Re} \left[ \mathbf{E} \times \boldsymbol{\Omega}_{\mathbf{k}}^{(0)} \right] + \tau e \int_{\mathbf{k}} \left\{ \text{Im} \left[ \nabla_{\mathbf{k}} \xi_{\mathbf{k}}^{(2)} + e\mathbf{E} \times \boldsymbol{\Omega}_{\mathbf{k}}^{(1)} \right] \cdot \nabla_{\mathbf{k}} f_0 \right\} \text{Re} \nabla_{\mathbf{k}} \xi_{\mathbf{k}}^{(0)} \\ &+ \tau^2 e^3 \int_{\mathbf{k}} \left\{ W^2 \mathbf{E} \cdot \nabla_{\mathbf{k}} \left[ \text{Im} \left( \mathbf{E} \times \boldsymbol{\Omega}_{\mathbf{k}}^{(0)} \right) \cdot \nabla_{\mathbf{k}} f_0 \right] + W^2 \text{Im} \left( \mathbf{E} \times \boldsymbol{\Omega}_{\mathbf{k}}^{(0)} \right) \cdot \nabla_{\mathbf{k}} \left[ \mathbf{E} \cdot \nabla_{\mathbf{k}} f_0 \right] \right\} \text{Re} \nabla_{\mathbf{k}} \xi_{\mathbf{k}}^{(0)} \\ &- \tau^2 e^3 \int_{\mathbf{k}} W^4 \text{Im} \left( \mathbf{E} \times \boldsymbol{\Omega}_{\mathbf{k}}^{(0)} \right) \cdot \nabla_{\mathbf{k}} \left[ \text{Im} \left( \mathbf{E} \times \boldsymbol{\Omega}_{\mathbf{k}}^{(0)} \right) \cdot \nabla_{\mathbf{k}} f_0 \right] \text{Re} \nabla_{\mathbf{k}} \xi_{\mathbf{k}}^{(0)}. \end{aligned} \right. \quad (\text{A32})$$

The expression for the second-order nonlinear DC conductivity is given by:

$$\begin{aligned}
\sigma_{\mu\nu\theta} = & \sigma_{\mu\nu\theta} (W = 0) + \tau e^3 W^2 \int_{\mathbf{k}} \frac{\epsilon_{i\nu l} \epsilon_{\mu\theta\gamma} \partial_i f_0 \text{Im}\Omega_l^{(0)} \text{Re}\Omega_\gamma^{(0)} + \theta \leftrightarrow \nu}{2} + \frac{(2\partial_\theta \text{Im}G_{\nu i}^{LR} - \partial_i \text{Im}G_{\nu\theta}^{LR}) \partial_i f_0 + \theta \leftrightarrow \nu}{2} \partial_\mu \text{Re}\xi_{\mathbf{k}}^{(0)} \\
& + \tau^2 e^3 W^2 \int_{\mathbf{k}} \frac{\epsilon_{j\theta i} \left( \partial_\nu \text{Im}\Omega_i^{(0)} \partial_j f_0 + 2\text{Im}\Omega_i^{(0)} \partial_j \partial_\nu f_0 \right) + \theta \leftrightarrow \nu}{2} \partial_\mu \text{Re}\xi_{\mathbf{k}}^{(0)} \\
& + \tau^2 e^3 W^4 \int_{\mathbf{k}} \frac{\epsilon_{i\nu j} \epsilon_{n\theta\gamma} \text{Im}\Omega_j \partial_i (\text{Im}\Omega_\gamma \partial_n f_0) + \theta \leftrightarrow \nu}{2} \partial_\mu \text{Re}\xi_{\mathbf{k}}^{(0)}
\end{aligned} \tag{A33}$$

In a two-dimensional nonHermitian system, the nonlinear DC conductivity becomes

$$\begin{aligned}
\sigma_{\mu\nu\theta} = & \sigma_{\mu\nu\theta} (W = 0) + \tau e^3 W^2 \int_{\mathbf{k}} \frac{\epsilon_{i\nu z} \epsilon_{\mu\theta z} \partial_i f_0 \text{Im}\Omega_z^{(0)} \text{Re}\Omega_z^{(0)} + \theta \leftrightarrow \nu}{2} + \frac{(2\partial_\theta \text{Im}G_{\nu i}^{LR} - \partial_i \text{Im}G_{\nu\theta}^{LR}) \partial_i f_0 + \theta \leftrightarrow \nu}{2} \partial_\mu \text{Re}\xi_{\mathbf{k}}^{(0)} \\
& + \tau^2 e^3 W^2 \int_{\mathbf{k}} \frac{\epsilon_{j\theta z} \left( \partial_\nu \text{Im}\Omega_z^{(0)} \partial_j f_0 + 2\text{Im}\Omega_z^{(0)} \partial_j \partial_\nu f_0 \right) + \theta \leftrightarrow \nu}{2} \partial_\mu \text{Re}\xi_{\mathbf{k}}^{(0)} \\
& + \tau^2 e^3 W^4 \int_{\mathbf{k}} \frac{\epsilon_{i\nu z} \epsilon_{n\theta z} \text{Im}\Omega_z \partial_i (\text{Im}\Omega_z \partial_n f_0) + \theta \leftrightarrow \nu}{2} \partial_\mu \text{Re}\xi_{\mathbf{k}}^{(0)}
\end{aligned} \tag{A34}$$

Specially,

$$\begin{aligned}
\sigma_{\mu\mu\mu} = & \sigma_{\mu\mu\mu} (W = 0) + \tau e^3 W^2 \int_{\mathbf{k}} (2\partial_\mu \text{Im}G_{\mu i}^{LR} - \partial_i \text{Im}G_{\mu\mu}^{LR}) \partial_i f_0 \partial_\mu \text{Re}\xi_{\mathbf{k}}^{(0)} \\
& + \tau^2 e^3 W^2 \int_{\mathbf{k}} \epsilon_{j\mu z} \left( \partial_\mu \text{Im}\Omega_z^{(0)} \partial_j f_0 + 2\text{Im}\Omega_z^{(0)} \partial_j \partial_\mu f_0 \right) \partial_\mu \text{Re}\xi_{\mathbf{k}}^{(0)} \\
& + \tau^2 e^3 W^4 \int_{\mathbf{k}} \epsilon_{i\mu z} \epsilon_{n\mu z} \text{Im}\Omega_z \partial_i (\text{Im}\Omega_z \partial_n f_0) \partial_\mu \text{Re}\xi_{\mathbf{k}}^{(0)}
\end{aligned} \tag{A35}$$

$$\begin{aligned}
\sigma_{xxx} = & \sigma_{xxx} (W = 0) + \tau e^3 W^2 \sum_{i \in x, y} \int_{\mathbf{k}} (2\partial_x \text{Im}G_{xi}^{LR} - \partial_i \text{Im}G_{xx}^{LR}) \partial_i f_0 \partial_x \text{Re}\xi_{\mathbf{k}}^{(0)} \\
& - \tau^2 e^3 W^2 \int_{\mathbf{k}} \left( \partial_x \text{Im}\Omega_z^{(0)} \partial_y f_0 + 2\text{Im}\Omega_z^{(0)} \partial_y \partial_x f_0 \right) \partial_x \text{Re}\xi_{\mathbf{k}}^{(0)} \\
& + \tau^2 e^3 W^4 \int_{\mathbf{k}} \text{Im}\Omega_z \partial_y (\text{Im}\Omega_z \partial_x f_0) \partial_x \text{Re}\xi_{\mathbf{k}}^{(0)}
\end{aligned} \tag{A36}$$

and

$$\begin{aligned}
\sigma_{yyy} = & \sigma_{yyy} (W = 0) + \tau e^3 W^2 \sum_{i \in x, y} \int_{\mathbf{k}} (2\partial_y \text{Im}G_{yi}^{LR} - \partial_i \text{Im}G_{yy}^{LR}) \partial_i f_0 \partial_y \text{Re}\xi_{\mathbf{k}}^{(0)} \\
& + \tau^2 e^3 W^2 \int_{\mathbf{k}} \left( \partial_y \text{Im}\Omega_z^{(0)} \partial_x f_0 + 2\text{Im}\Omega_z^{(0)} \partial_x \partial_y f_0 \right) \partial_y \text{Re}\xi_{\mathbf{k}}^{(0)} \\
& + \tau^2 e^3 W^4 \int_{\mathbf{k}} \text{Im}\Omega_z \partial_x (\text{Im}\Omega_z \partial_y f_0) \partial_y \text{Re}\xi_{\mathbf{k}}^{(0)}
\end{aligned} \tag{A37}$$

$$\begin{aligned}
\sigma_{xyy} = & \sigma_{xyy} (W = 0) + \tau e^3 W^2 \int_{\mathbf{k}} \partial_x f_0 \text{Im}\Omega_z^{(0)} \text{Re}\Omega_z^{(0)} + \sum_{i \in x, y} (2\partial_y \text{Im}G_{yi}^{LR} - \partial_i \text{Im}G_{yy}^{LR}) \partial_i f_0 \partial_x \text{Re}\xi_{\mathbf{k}}^{(0)} \\
& + \tau^2 e^3 W^2 \int_{\mathbf{k}} \left( \partial_y \text{Im}\Omega_z^{(0)} \partial_x f_0 + 2\text{Im}\Omega_z^{(0)} \partial_j \partial_y f_0 \right) \partial_x \text{Re}\xi_{\mathbf{k}}^{(0)} \\
& + \tau^2 e^3 W^4 \int_{\mathbf{k}} \text{Im}\Omega_z^{(0)} \partial_x (\text{Im}\Omega_z^{(0)} \partial_x f_0) \partial_x \text{Re}\xi_{\mathbf{k}}^{(0)}
\end{aligned} \tag{A38}$$